Differences between FRP bond behavior in cracked and uncracked regions

M. Taher Khorramabadi and C.J. Burgoyne

Synopsis: Based on an analysis of the experimental results of a proposed bond test method, significant differences are shown to exist between the local FRP bond stress-slip relationships in the uncracked anchorage regions and in the regions between cracks. The proposed method simulates the bond behavior between the flexural cracks and anchorage regions of a flexurally FRP-strengthened RC beam. The boundary conditions, including the presence of cracks and steel, are shown to have significant effects on the local bond stress-slip models. The results showed that, at the same force, the bond stresses in the regions between cracks were lower than in regions outside the cracks, so the debonding formed in the anchorage regions. The local bond stress-slip models in the anchorage regions can be obtained from the conventional bond test methods but these do not mimic the conditions between the cracks.

Keywords: anchorage region, average bond stress-slip model, bond behavior, cracked region, local bond stress-slip model

M. Taher Khorramabadi:
PhD candidate, Department of Engineering, University of Cambridge, UK

C.J. Burgoyne:
Reader in Concrete Structures, Department of Engineering, University of Cambridge, UK

INTRODUCTION

Fiber Reinforced Polymers (FRP) have been widely used for flexural strengthening of Reinforced Concrete (RC) beams. Flexural strengthening can be achieved by epoxy-bonding FRP sheets, strips, or bars to the tension side of the members. If the FRP is applied on the surface of the beam the method is called Externally Bonded (EB) reinforcement, while if placed in a groove the method is referred to as Near Surface Mounted (NSM). The strengthening depends on the effective stress transfers between FRP and concrete that is a key to the overall behavior of the strengthened beams. Present paper distinguishes between the bond behavior in the anchorage region, where FRP is pulled from one end and is free from other end, and the cracked region, where FRP is pulled from both ends, of a strengthened beam. Figure 1 shows part of an RC beam strengthened with NSM FRP reinforcement in a four point bending configuration between a support and mid span, in which the anchorage and cracked regions are shown.

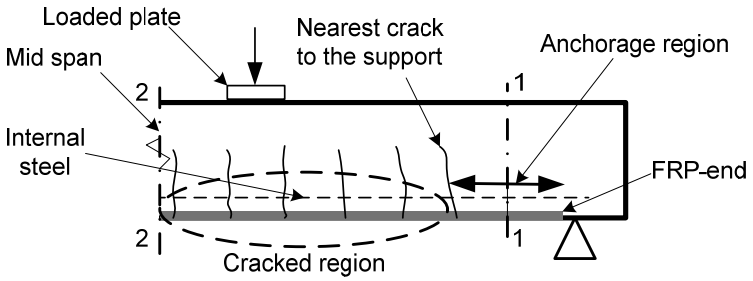

Figure 1 — Half of a strengthened RC beam with flexural cracks

There are many different experimental set-ups for determining the bond behavior of the FRP-concrete, that here are referred to as conventional bond tests, amongst which single shear bond tests (Taljsten, 1997;Bizindavyi et al., 1999;Teng et al., 2006), double shear bond tests (Yoshizawa et al., 2000;Yan et al., 1999), and shear bending bond tests (De Lorenzis et al., 2001;De Lorenzis et al., 2001;De Lorenzis et al., 2002) are the most common. The first two test set-ups are direct pullout tests as the FRP is directly pulled out from the concrete block by a tensile force (shown in Figure 2). Figure 3 shows the bond tests in the form of beams, where the load is applied directly to the beams.

Double-shear pull tests and single-shear pull tests have been the most popular test methods, as a result of their simplicity (Chen et al., 2001). Numerical and experimental studies have shown that different test set-ups can lead to significantly different test results and small variations in set-up (for instance the height of the support block in a single or double-shear push tests) may have significant effects (Yao et al., 2005). This shows that the stress field in the concrete induced by the support can affect the results of the bond tests and means that the boundary conditions of the system may alter the results. Thus, bending bond tests (Figure 3) are more likely to represent the actual conditions than the direct pullout tests. However, in both cases, concrete cracks perpendicular to the bonded FRP are avoided where possible. Thus, even in the bending bond tests, the FRP is pulled from one end and is free at the other end, with no crack along the bonded length. This will be termed *anchorage region conditions*. Therefore, almost all conventional bond tests effectively simulate the conditions in the anchorage region and not in the cracked regions of a strengthened beam.

The other difference between the anchorage and cracked regions of a strengthened RC beam is that the internal steel strain in the cracked regions is usually higher than in the anchorage regions. Taher and Burgoyne (Taher Khorramabadi et al., 2009) showed that the steel presence significantly alters the average FRP-concrete bond stress-slip relationship. A bond test method was proposed that accounts for the steel effects (pre-/post-yielding), as well as complying with the actual boundary conditions in the cracked and anchorage regions in a single specimen. The specimens were designed as concrete ties subjected to pure tension which were reinforced internally with steel and strengthened with Near Surface Mounted (NSM) CFRP strips.

In this paper, the boundary conditions in the cracked and anchorage regions are compared. A brief introduction to the proposed bond test method of Taher and Burgoyne (Taher Khorramabadi et al., 2009) is given. The local bond stress-slip relationships for both cracked and anchorage regions are obtained experimentally. The results show that the local bond behavior differs significantly in the anchorage and cracked regions and that the steel strains affect the bond behavior. The research shows that a different type of behavior occurs in the two regions, which can only be observed by a test of the sort proposed here.

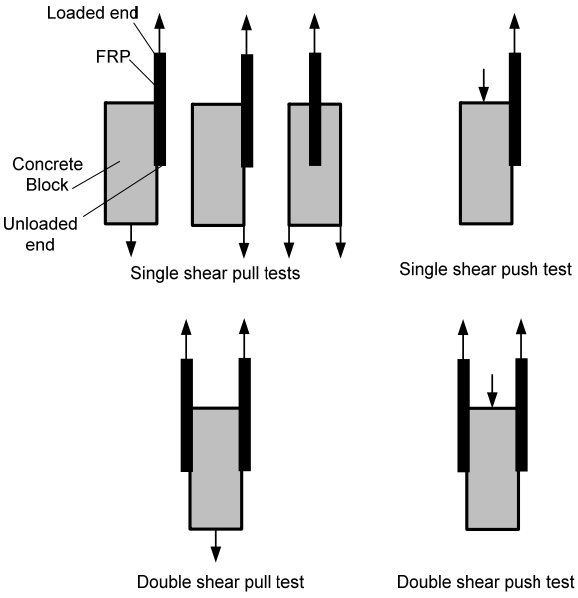

Figure 2 — Direct pull out tests set-ups

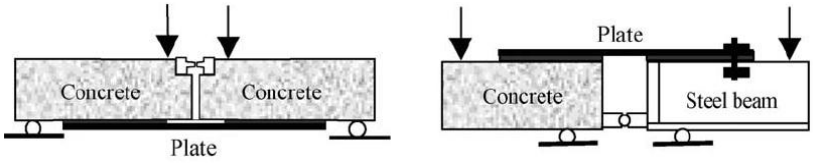

(a) Beam test (b) Modified beam test

Figure 3 — Classification of beam set-up bond tests (Yao et al., 2005)

BOND BEHAVIOR IN THE CRACKED AND ANCHORAGE REGIONS

The mechanism of cracking and bond behavior between two cracks can most easily be understood by considering a reinforced concrete member subjected to pure tension. Figure 4a shows the area between two preformed cracks in such a member reinforced with steel & FRP. The applied load T is carried partly by the concrete, partly by the steel and also by the FRP strip. The proportions vary with the distance from the cracked section x. At the crack, no load is carried by the concrete. Away from the crack, the load in the reinforcement decreases. At a distance L_t (transfer length) away from the crack, the strain in the reinforcement (steel & FRP) is equal to the concrete strain beyond which the slip and bond stress between the reinforcement and the concrete is zero. The strain, slip, and bond stress distributions before formation of the first crack in the concrete and the FRP are shown in Figure 4a. It should be noted that the transfer lengths for FRP and steel may differ. As the load T increases, new cracks form when the

concrete strain exceeds its cracking strain. The number of cracks increases in this way to reach a stabilized strain condition.

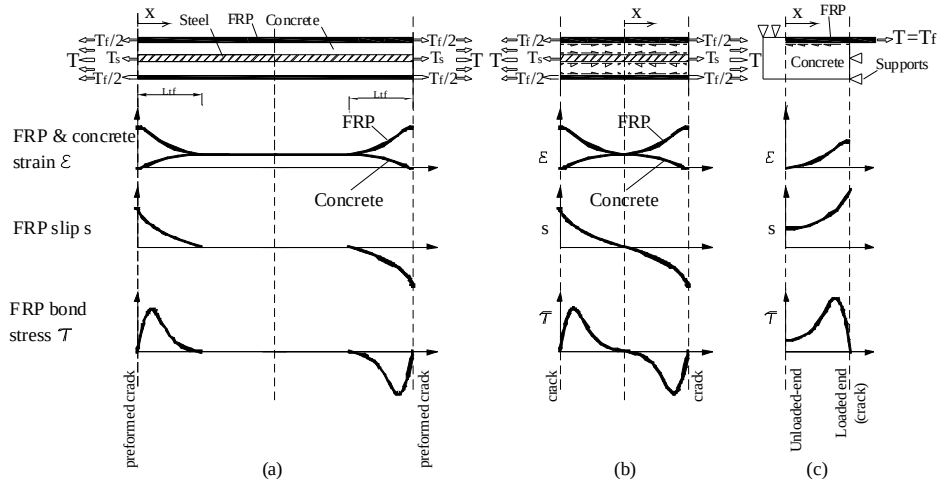

Figure 4 — Strain, slip, and bond stress distributions (a)before cracking load between two cracks (proposed test method) (b) between two cracks at final cracking stage (proposed test method) (c) in anchorage region (conventional bond test)

The FRP strain, slip, and bond stress distributions between two final cracks are shown in Figure 4b. At the cracked sections, the tension is carried by the FRP and the steel alone and the strains in the reinforcement attain maximum values. Between cracks, the concrete carries some tension and there is a corresponding reduction in the reinforcement stresses. As a result, the bond must take the stress out of the reinforcement adjacent to a crack and put it back in before the next crack is reached. Between adjacent cracks, the directions of the bond stress and slip reverse and at one point at least, the bond stress and slip must be zero.

As mentioned earlier, the conventional way to test the bond properties of reinforcement is to pull a bar from a concrete block (shown in Figure 4c). The differences between bond behavior in Figure 4b&c are clear. In the conventional bond tests, a stress distribution forms with a maximum close to the loaded end and zero at the unloaded end (FRP-end). The FRP-end slip is initially zero, but eventually slip propagates through from the loaded end even though there is no strain at the FRP-end. This differs from the conditions between the two cracks, where slip remains zero at one point between the two cracks. Bond stress in a conventional test is initially zero away from the loaded end, but eventually stresses develop as the strain propagates through from the loaded end. Considering that strain at the FRP-end is always zero, the strain difference between the FRP-end and a nearby point produces bond stress in the region close to the FRP-end. This condition is not the same as in the regions between cracks since there is a point between the cracks at which the bond stress is always zero, where the direction of the bond stress

changes. Thus, the conventional test does not provide boundary conditions that mimic the behavior between cracks.

In the cracked regions of a strengthened RC beam close to mid span, the internal steel strain is higher and the steel is more likely to yield than in the anchorage regions. The FRP is being provided to enhance the tensile capacity of a beam, which is presumably deficient. The main tension steel is likely to be at a cover depth in from the surface, and the NSM reinforcement is placed in a groove cut in that cover. The presence of steel is known to affect the strain distribution in concrete (which is why steel is detailed to control the crack widths in beams and slabs). Thus, the strain in the concrete next to the FRP is likely to be affected by the nearby rebar, which is not taken into account in a conventional bond test.

EXPERIMENTAL INVESTIGATION

The proposed bond test method by Taher and Burgoyne (Taher Khorramabadi et al., 2009) mimics the conditions in the anchorage and cracked regions of an FRP-strengthened RC beam. The specimens consisted of uniaxial tensile tests on RC ties strengthened with NSM FRP strips, shown in Figure 5. Three preformed notches were located along the bond specimens to simulate the flexural cracks of a beam. The distances between the notches were chosen to ensure that no crack formed up to the designed failure load. The regions between the notches (*central regions*) simulated the conditions between the cracked regions in the beams. The regions between the end notches and the specimen ends (*anchorage regions*) had similar conditions to a conventional double shear bond specimen and the anchorage region of a beam.

Two out of five bond test specimens in those experiments will be considered in this study. The specimens were reinforced with the FRP strips (1.2 mm×12 mm or 0.05in.×0.47in.), embedded in the cast-in 5 mm×14 mm (0.2in.×0.6in.) grooves, filled with epoxy on two opposite faces of the concrete ties along their full length. The anchorage regions were reinforced internally with two 16 mm (0.6in.) plus one 10mm (0.4in.) steel bars. The 10mm (0.4in.) steel bar was continued along the full length of the specimen with steel in the central region. As a result of increasing the steel percentage in the end regions compared to the central region, it becomes possible for the central steel to yield. Therefore, the load increment would be carried only by the CFRP at the cracked section, and by the concrete, CFRP, and steel (if locally unyielded) between two notches. The specimens were placed in a 2000kN (450kip) test machine. The connection to the testing machine was via the extended anchorage steel bars, which were pulled until specimens failed.

The FRP and the central steel strains were locally measured by strain gauges; the location of the gauges is shown in Figure 5. The FRP-end displacements were monitored by displacement transducers, the total pull-out force was measured by a load

cell, and the relative displacement between the grips was measured by a built-in displacement transducer. The material properties are presented in Table 1.

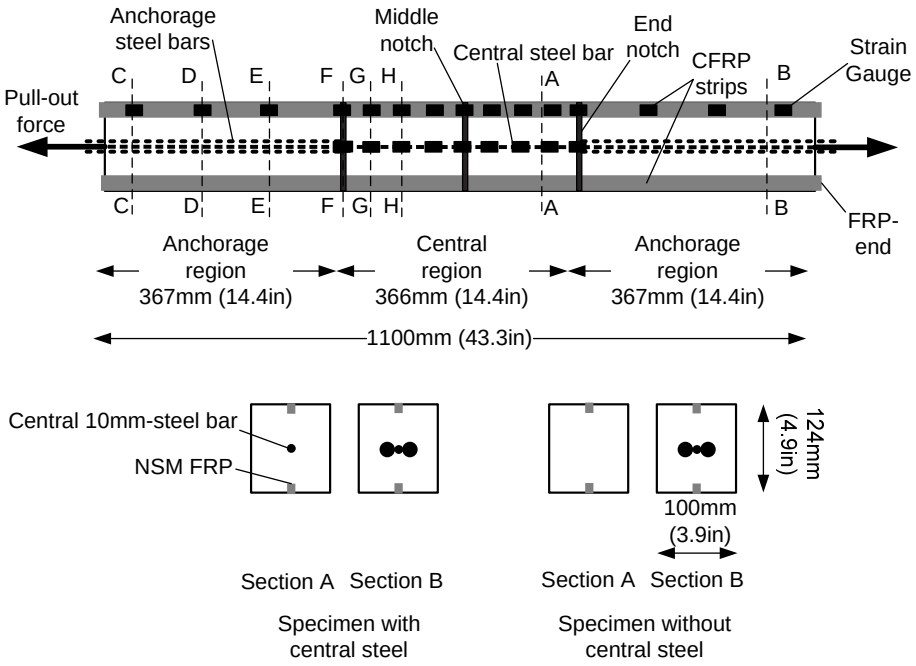

Figure 5 — Bond test specimens

Table 1 — Material properties

Concrete cube strength, specimen with central steel	92 MPa (13.3 ksi)
Concrete cube strength, specimen without central steel	73 MPa (10.6 ksi)
Concrete Young's modulus	35 GPa (5080 ksi)
FRP Young's modulus	165 GPa (23900 ksi)
Steel Young's modulus	200 GPa (29000 ksi)
FRP ultimate strength	2800 MPa (406 ksi)
Steel yielding strength	600 MPa (87 ksi)

Observed failure mode

Figure 6 shows the overall behavior of the specimens in terms of external load against total elongation of the specimens. The elongation is measured from the displacement between the two grips; therefore the possible slip between grips and the anchorage steel bars is included in these values. Figure 7 shows the specimens after failure.

The initial response of the specimen with central steel was generally linearly-elastic until the preformed notches opened at about 30kN (6.7kips), and remained linear until the central steel yielded at about 60kN (13.5kips) when the stiffness further reduced. The response became nonlinear at about 70kN (15.7kips) when herringbone cracks initiated mainly in the central region. At about 76kN (17.1kips) diagonal cracks formed in the anchorage region close to the end notches. Subsequently, the debonding propagated from the toe of the secondary cracks towards the specimen's end in the top anchorage region, shown in Figure 7a. The specimens failed as debonding reached the FRP-end at about 90kN (20.2kips) load.

The response of the specimen without central steel was linear-elastic up to opening of the middle notch at about 20kN (4.5kips). The herringbone crack formation started at about 24kN (5.4kips) in the central region. The response became nonlinear as diagonal secondary cracks formed in the anchorage region close to the end notches and debonding initiated from the secondary crack toes, primarily in the FRP-epoxy interface but also in the epoxy-concrete interface at about 43kN (9.7kips), shown in Figure 7b. The debonding propagated into the anchorage region and the specimen failed at 51 kN (11.5kips).

Both specimens failed immediately as the FRP-end slipped into the specimens, and therefore, no FRP-end slip was measured by the displacement transducers.

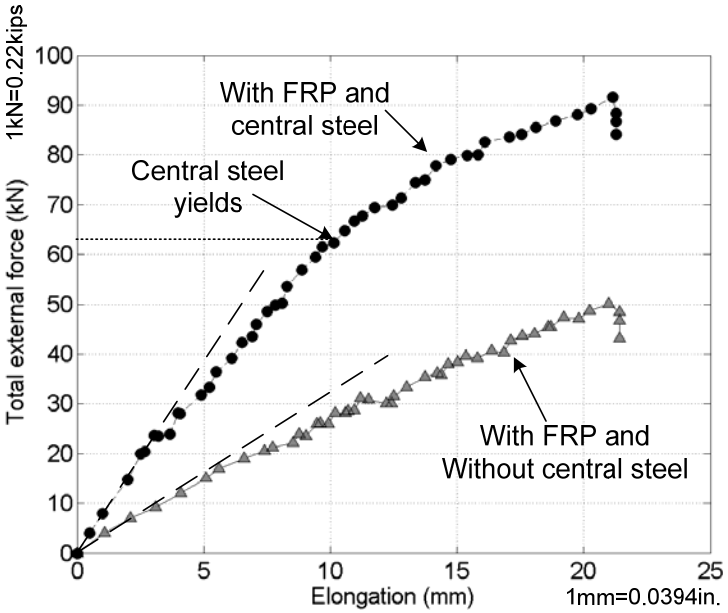

Figure 6 — Overall behavior of the bond specimens

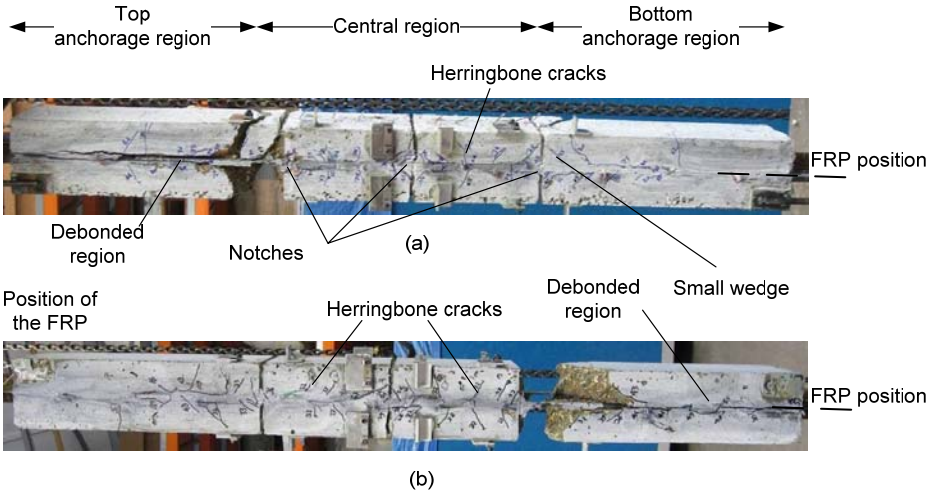

Figure 7 — Specimens after failure (a) specimen with FRP & central steel (b) specimen with FRP and no central steel

LOCAL BOND STRESS-SLIP RELATIONSHIP

Governing bond differential equation (Eq. 1) of a bonded FRP to concrete of length dx can be derived from the equilibrium and compatibility equations that relates the second order derivative of the slip (s) to the local bond stress (τ).

$$\frac{d^2 s(x)}{dx^2} = \frac{\Sigma_p}{EA}\tau \qquad \text{Eq. 1}$$

where E and A are the modulus of elasticity and the cross-sectional area of FRP, respectively. Σ_p is effective perimeter of the section at which the bond stress is calculated.

The following four assumptions have been made in order to solve the bond equation (Eq. 1):

- FRP has a linear elastic material law in the longitudinal direction.
- The displacement of the FRP is significantly higher than the concrete at the FRP-concrete interface.
- The stiffness of the epoxy is negligible in comparison to the FRP
- There exists a bond characteristic at the FRP-concrete interface that can be analytically described by a relationship between the local bond stress acting at the interface, and the slip between FRP and concrete (Tassios et al., 1981;George Nammur Jr. et al., 1989;Lees et al., 1999;Focacci et al., 2000).

The solution of the governing bond equation depends on the boundary conditions and the assumed form of the $\tau - s$ relationship. The assumed bond model in this paper is shown in Figure 8, which can be defined with Eq. 2 & Eq. 3.

$$\tau = \tau_m \left(\frac{s}{s_1}\right)^{\alpha} \qquad s \le s_1 \qquad \text{Eq. 2}$$

$$\tau = \tau_m \left(\frac{s}{s_1}\right)^{\alpha'} \qquad s > s_1 \qquad \text{Eq. 3}$$

where s_1 is the slip at which the maximum bond stress τ_m occurs. The exponents α , α' reflect the shape of the bond stress-slip distributions.

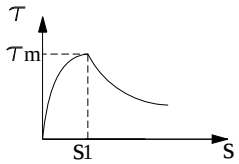

Figure 8 — Assumed bond stress-slip model

Eq. 2 is the ascending branch of the well known BPE model (Eligehausen R. et al., 1983) which originally was proposed for modeling the $\tau - s$ relationship of a steel bar to concrete. Eq. 3 is identical to Eq. 2, with exception that exponent α' is negative as proposed by de Lorenzis (De Lorenzis et al., 2002). She modeled the descending branch of the $\tau - s$ relationship of a Glass Fiber Reinforced Polymer (GFRP) ribbed bars which failed at the epoxy–concrete interface. Eq. 3 corresponds to an ever-decreasing zero for infinite values of slip.

Eq. 2 & Eq. 3 have been used previously by Cruz (Cruz et al., 2004) for specimens that failed either in the concrete-adhesive or in the adhesive-laminate interfaces, good fits were obtained with their experimental results.

The boundary conditions that can be implanted to solve the bond equation (Eq. 1) depend on the type of the problem and the available experimental data. For these experiments, Eq. 4 shows the chosen boundary conditions in the central region of the bond specimens; the slip is zero midway between the cracks ($x = 0$ in Figure 4b or Section G-G in Figure 5) and the strain ε_0 at this point has been measured with a strain gauge.

$$\begin{cases} \varepsilon(x=0) = \dfrac{ds}{dx}(0) = \varepsilon_0 \\ s(x=0) = 0 \end{cases} \qquad \text{Eq. 4}$$

The boundary conditions in the anchorage regions can be defined as strain and slip at one point of the bonded length with Eq. 5:

$$\begin{cases} \varepsilon(x_i) = \varepsilon_i \\ s(x_i) = s_i \end{cases} \qquad \text{Eq. 5}$$

where, ε_i and s_i are the measured strain and slip at point i, respectively. x_i is the location of a strain gauge that is away from the cracked section. The slip can be calculated by integrating the FRP strain from the FRP-end up to strain gauge i. For

instance, at Section $E-E$ in Figure 5, ε_i and s_i were the measured strain and slip at point E ,respectively. The strain was measured directly by strain gauges at E and the slip was calculated from the strain integration along CE plus the measured slip at the FRP-end from the transducer. In calculating the slip, it is assumed that the strain between each pair of the strain gauges varies linearly.

So far, the boundary conditions and the form of the $\tau - s$ are defined. The four unknown parameters $(\tau_m, s_1, \alpha, \alpha')$ of the $\tau - s$ relationship can be found from the solution of the bond equation Eq. 1 through an optimization process. Since it is assumed that the local $\tau - s$ relationship is unique, the solution of the bond equation has to be valid for any point along the bonded length. Therefore, in each iteration, the solution of the bond equation will be checked with the measured strains at different points. This has been done by defining an error function. The best set of the four parameters that minimizes the error function is chosen as the local bond stress-slip model.

For the central region, the error function was defined as the sum of the squares of the difference between the measured and theoretical strains (solution of the bond equation) at the neighboring strain gauge and at the cracked sections. These are the points at which the strains were measured experimentally.

For example, along the bonded length segment HGF in Figure 5 the error function was defined as:

$$Er = \sum_{i=1}^{n} \left[2\left(\left(\varepsilon_{Gi}\right)_{exp} - \left(\varepsilon_{Gi}\right)_{theo} \right)^2 + \left(\left(\varepsilon_{Fi}\right)_{exp} - \left(\varepsilon_{Fi}\right)_{theo} \right)^2 \right] \qquad \text{Eq. 6}$$

where, n is the number of the available data at each point, subscripts exp and $theo$ stand for experimental and theoretical data, respectively. Since point G was located midway between F and H , the effect of point G was given increased weighted by a factor of 2 .

In the anchorage regions, the error function was defined as the square of the difference between the experimental and theoretical strain at the neighboring strain gauge closer to the cracked section. For example, along the segment DE the measured strain at D was taken as one of the initial boundary conditions (Eq. 5) and the measured strain at E is applied into the error function:

$$Er = \sum_{i=1}^{n} \left(\left(\varepsilon_{Ei}\right)_{exp} - \left(\varepsilon_{Ei}\right)_{theo} \right)^2 \qquad \text{Eq. 7}$$

Experimental local bond stress-slip results

Based on the method described in the previous section, the parameters of the assumed local FRP bond stress-slip models (Eq. 2 and Eq. 3) in the central regions with and without steel and in the anchorage regions were found at the epoxy-concrete interface. Table 2 presents the average values from four regions of the specimen with steel and two regions of the specimen without steel. The average curves are plotted in Figure 9. It is argued in Taher Khorramabadi (2010) that there is a unique bond stress-slip relationship in the regions with the same boundary conditions and these average values are good representations of the bond behavior of the regions.

Table 2 —Experimental FRP-concrete local bond stress-slip parameters

Specimen Type	τ_m MPa (ksi)	s_1 mm $(in.)$	α	α'	Er (10^{-4})	Area under curves D_L* N/mm $(lb/in.)$
Central region with FRP and Steel	3.63 (0.53)	0.056 (0.0022)	0.736	-0.390	1.29	1.72 (9.81)
with FRP	2.99 (0.43)	0.0481 (0.0019)	0.343	-0.456	1.17	1.22 (6.96)
Anchorage regions	9.05 (1.31)	0.290 (0.011)	0.172	-1.674	0.30	4.42 (25.2)

* D_L is the area below each curve in Figure 9.

The effects of steel presence can be studied by comparing the results from specimens with and without steel in the central region. It can be seen that at the same slip, local bond stresses in the specimen with steel are higher than the local bond stresses in the specimen with only FRP.

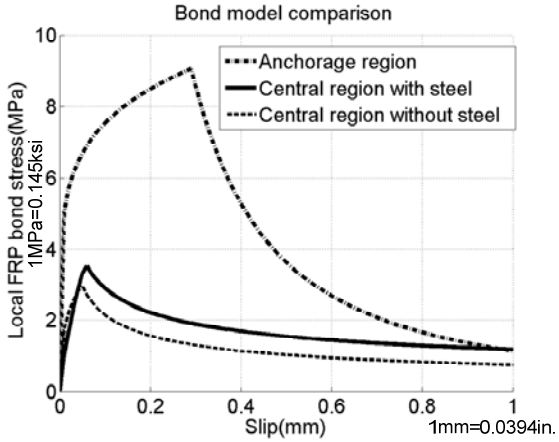

Figure 9 — Comparison between the experimental local bond models

The specimen without steel had slightly higher initial stiffness compared to the specimen with steel. However, its stiffness gradually decreased as it reached the peak stress. The peak bond stress in specimen with steel was about 3.6MPa (0.52ksi) at the slip of 0.06mm (0.0023in.). Peak bond stress and slip values were higher than in the specimen without steel in which the peak stress was 3.00MPa (0.44ksi) at 0.05mm (0.002in.). Beyond their peak stresses, bond stresses gradually decreased as the slip increased.

The local peak bond stresses in the anchorage regions was about 9MPa (1.3ksi) which was about three times higher than the values obtained in the central region. The slip s_1 at which the peak bond stress was observed in the anchorage region was about 0.3mm (0.0118in.) while that observed in the central region was about 0.05mm (0.002in.).

The area below the curves represents the dissipated energy D_L at the interface, tabulated in Table 2. The dissipated energy in the specimen with steel was about 40% higher than in without steel. At the same value of FRP slip in the anchorage region, D_L was more than 150% and 260% higher than the central regions with steel and without steel, respectively.

The descending branch in the anchorage region initiated as a result of debonding at the epoxy-concrete interface, whereas in the central regions it initiated as a result of reduction in the stiffness at the interface due to formation of the herringbone cracks in the nearby concrete before the bond stresses exceeded its debonding strength. The bond behavior at different regions in the same specimens depended on the presence of the preformed cracks. The crack presence altered the boundary conditions and consequently the local bond behavior.

The results show that the bond models obtained from the anchorage regions of the proposed method (similar to conventional pull-out tests) do not reflect bond characteristics in the cracked regions, and overestimate bond strength. The Japan Society of Civil Engineers stated that the pull-out tests given in JSCE (JSCE-E 539, 1995) are incapable of measuring bond strength accurately, owing to differences in the stress conditions in actual members. The pull-out test referred to is the test method for determining the bond strength of Continuous Fiber Reinforcing Material (CFRM) used in place of steel reinforcement or pre-stressing tendon in concrete by pull-out testing. In this test method, the tendon with a minimum length of four times its diameter is placed at the centre of a cubic or cylindrical concrete specimen, and tendons are pulled out while constraining the specimen at the loaded face.

CONCLUSION

Based on the force transfer mechanism, it was shown that the boundary conditions in the cracked regions differ from the anchorage regions, where the reinforcement is pulled from one end only.

In the present work, the local bond stress-slip models for different regions were found experimentally. The results show that the local bond behavior depends on the boundary conditions. Different boundary conditions, including the presence of cracks and steel were investigated in this study. The bond behavior between the cracks showed lower bond strength due to formation of herringbone cracks and debonding did not form in these regions, although the FRP strain was high enough to cause debonding in the anchorage regions in the same specimen. The presence of steel increased slightly the bond strength in the cracked regions, and increased the dissipated energy at the interface by about 40% when compared with the region without steel.

In conclusion, the boundary conditions of the implemented bond models have to comply with the actual boundary conditions of the problem and it is insufficient to treat the bond strength as a material property that is independent of the geometry and the actual boundary conditions. The bond models inherently represent the structural behavior of the systems from which they have been derived. Therefore, a true material property (e.g. bond-stress slip model or dissipated energy) can only be obtained when the actual boundary conditions are considered.

Acknowledgment

The financial support of Cambridge Overseas Trust and Cambridge Overseas Research Studentship are gratefully acknowledged.

References

1. Taljsten,B. (1997). Defining anchor lengths of steel and CFRP plates bonded to concrete. International Journal of Adhesion and Adhesives 17**,** 319-327.

2. Bizindavyi,L., and Neale,K.W. (1999). Transfer lengths and bond strengths for composites bonded to concrete. Journal of Composites for Construction 3**,** 153-160.

3. Teng,J.G., De Lorenzis,L., Wang,B., Li,R., Wong,T.N., and Lam,L. (2006). Debonding failures of RC beams strengthened with near surface mounted CFRP strips. Journal of Composites for Construction 10**,** 92-105.

4. Yoshizawa,H., Wu,Z., Yuan,H., and Kanakubo,T. (2000). Study on FRP-concrete interface bond performance. Trans. Japan Society of Civil Engineers 662**,** 105-119.

5. Yan, X., Miller, B., Nanni, A., and Bakis, C. E. Characterization of CFRP bars used as near-surface mounted reinforcement. 8th International Structural Faults and Repair Conference . 1999. Edinburgh, Scotland, Engineering Technics Press.

6. De Lorenzis,L., Miller,B., and Nanni,A. (2001). Bond of fiber-reinforced polymer laminates to concrete. ACI Materials Journal 98**,** 256-264.

7. De Lorenzis,L., and Nanni,A. (2001). Characterization of FRP rods as near-surface mounted reinforcement. Journal of Composites for Construction 5**,** 114-121.

8. De Lorenzis,L., and Nanni,A. (2002). Bond between near-surface mounted fiber-reinforced polymer rods and concrete in structural strengthening. ACI Structural Journal 99**,** 123-132.

9. Chen,J.F., Yang,Z.J., and Holt,G.D. (2001). FRP or steel plate-to-concrete bonded joints: effect of test methods on experimental bond strength. Steel Compos Struct 1**,** 231-244.

10. Yao,J., Teng,J.G., and Chen,J.F. (2005). Experimental study on FRP-to-concrete bonded joints. Composites Part B: Engineering 36**,** 99-113.

11. Taher Khorramabadi, M. and Burgoyne, C. J. Tests on FRP-concrete bond behaviour in the presence of steel. Halliwell, S., Whysall, C., and Stratford, T. Advanced Composites in Construction (ACIC) Conference Proceedings . 9-1-2009.

12. Tassios,T.P., and Yannopoulos,P.J. (1981). Analytical studies on reinforced concrete members under cyclic loading based on bond stress-slip relationships. ACI Journal Proceedings 78**,** 206-216.

13. George Nammur Jr., and Antoine E.Naaman (1989). Bond stress model for Fiber Reinforced Concrete based on bond stress-slip relationship. Materials Journal 86**,** 45-57.

14. Lees,J.M., and Burgoyne,C.J. (1999). Transfer bond stresses generated between FRP tendons and concrete. Magazine of Concrete Research 51**,** 229-239.

15. Focacci,F., Nanni,A., and Bakis,C.E. (2000). Local bond-slip relationship for FRP reinforcement in concrete. Journal of Composites for Construction 4**,** 24-31.

16. Eligehausen R., Popov E.P., and Bertero V.V. Local bond stress-slip relationships of deformed bars under generalized excitations. UCB/EERC-83/23, -169. 1983. University of California, Berkeley, Earthquake Engineering Research Center.

17. De Lorenzis,L., Rizzo,A., and La Tegola,A. (2002). A modified pull-out test for bond of near-surface mounted FRP rods in concrete. Composites Part B: Engineering 33**,** 589-603.

18. Cruz,J.M.S., and Barros,J.A.O. (2004). Bond between near-surface mounted carbon-fiber-reinforced polymer laminate strips and concrete. Journal of Composites for Construction 8**,** 519-527.

19. Taher Khorramabadi, M. FRP bond behaviour during intermediate concrete cover separation in flexurally strengthened RC beams. 2010. PhD thesis, University of Cambridge.

20. JSCE-E 539 (1995). Test method for bond strength of continuous fiber reinforcing material by pull-out testing. (Tokyo, Japan: Japan Society of Civil Engineers).